Nanocellulose films as substrates for printed electronics*

A. Pammo, H. Christophliemk, J. Keskinen, T. Björkqvist, S. Siljander, M. Mäntysalo and S. Tuukkanen

***Abstract*— Microfibrillated cellulose (MFC) was fabricated from cellulose pulp using in-house mechanical fibrillation equipment. Subsequently, free-standing MFC films were fabricated with in-house developed hot-plate drying technique. MFC films were tested as substrate materials for printed electronics patterns. Conducting patterns were fabrication on MFC film using different methods, such as screen printing and vacuum evaporation. Electrical conductivity of the fabricated patterns was measured using four-electrode technique. The MFC films showed their applicability and required stability to be used as a substrate material for printed functional patterns from electronic inks and thermal curing of the patterns.**

Keywords—nanocellulose, printed electronics, graphite ink

I. Introduction

Carbon based nanomaterials, also known as nanocellulose, is a group of sustainable, renewable, strong, lightweight, high surface area materials. Due to its extraordinary properties, nanocellulose has established a lot of interest in many different field of applications, such as construction materials, electronic components [1, 2], sensors [3, 4, 5] and biomedical applications [6]. Nanocellulose is a large set of materials which contain plant or bacterial based cellulose which dimensions are in the nanoscale. Nanofibrillated cellulose (NFC) is generally produced from wood-based cellulose using mechanical processing or/and chemical treatment to open the cellulose fibers structures into smaller fibrils, obtaining finally the nanoscale dimensions. Microfibrillated cellulose (MFC) is generally known also as one group of nanocellulose material, but it also contains some amount cellulose fibrils, which dimensions are above the nanoscale.

A controlled fabrication of free-standing MFC films is a challenge due to the special properties of cellulosic nanomaterials. There are only a few realized techniques for fabrication of films from MFC or NFC [3, 7].

*Research supported by Council of Tampere Region.

A. P. and S. T. are with the Tampere University, Faculty of Medicine and Health Technology, FI-33720 Tampere, Finland (corresponding author phone and E-mail: +358-40-541-5276, sampo.tuukkanen@tuni.fi) (E-mail: arno.pammo@tuni.fi).

H. C., J. K. and M. M. are with the Tampere University, Faculty of Information Technology and Communication Sciences, FI-33720 Tampere, Finland (E-mails: hanna.christophliemk@tuni.fi, jari.keskinen@tuni.fi, matti.mantysalo@tuni.fi).

T. B. and S. S. are with the Tampere University, Faculty of Engineering and Natural Sciences, FI-33720 Tampere, Finland (E-mails: tomas.bjorkqvist@tuni.fi, sanna.siljander@tuni.fi).

Printed electronics is proposed as a sustainable, more environmentally friendly alternative for conventional microfabrication techniques. However, there are quite many obstacles to be solved related to set of printable materials and substrates. Generally, oil-based plastics have been used as substrate materials for producing printed flexible electronic components and circuits. Nanocellulose is a promising sustainable material to be used as substrate for disposable electronics products, such as one-use point-of-care sensors.

In this paper, we describe the developed mechanical fibrillation methods for preparation of MFC gel, and subsequent fabrication of MFC films using hot-plate evaporation technique. The prepared films are utilized as a substrate material for conducting patterns and printed electronics.

II. Materials and Methods

A. Preparation of microfibrillated cellulose (MFC)

A1. Cellulose pretreatment

Nordic bleached hardwood kraft pulp was refined in an LC refiner. The refined pulp was then fractionated. The fine fraction, namely accept, was dewatered and stored at 25% consistency, whereas the reject fraction was not used in this study. The fine fraction contained 40% of fines (BMN -200) and was used as raw material for microfibrillation.

A2. Cellulose microfibrillation

The fibrillation was performed with an in-house built mechanical laboratory scale fibrillator. The construction is disc refiner type but with different plates compared to plates used in high or low consistency refining. Both the 110 mm outer diameter rotor and stator fibrillation surfaces are solids with roughness in µm scale and has now bars, grooves or dams. The cellulose fibers brought into the gap between the plates are exposed to mechanical shear and fiber structures are opened to fibril structures.

For the fibrillation stages, the pulp was diluted to 1.8 % consistency. The rotation speed of the rotor was 4880 rpm, and the axial closing force of the plate gap was adjusted to keep the feeding pressure roughly at 4 bar. The plate gap was gradually reduced at each stage by lowering the feeding rate. The three first stage were kept partly as homogenization stages, because mixing in the feeding tank remained incomplete and relatively little energy was applied. The succeeding three stages changed visually the pulp from a water suspension to a gel-like substance. The

Figure 1: *Photographs of prepared MFC gel.*

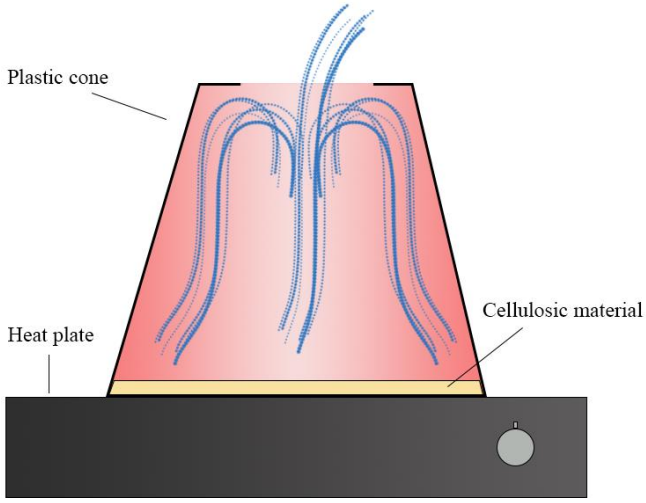

Figure 2: *MFC film drying-setup. The cone keeps some of the humidity inside which prevents MFC from drying unevenly.*

last fibrillation stage was run with 250 ml/min feeding rate, which serves as a measure of fibrillation state. A photographs if obtained MFC gel is shown in the Figure 1.

B. Fabrication of MFC films

Prepared raw 1.8 wt-% MFC gel (in water) was weighed in quantity of 250 g in order to produce films of different thicknesses. It was then diluted with deionized water in 2:1 water-to-MFC ratio and mixed thoroughly. Any air bubbles inside the solution were removed with vacuum suction technique. Obtained homogenous solution was poured on a polyethylene terephthalate (Polyethylene terephthalate, 125-µm-thick PET Melinex ST506) substrate placed on a hot plate inside the area enclosed by a plastic cone. Dilution of MFC before film formation was done to obtain more evenly distributed MFC films. Hot plate temperature was set to 50 °C and the material was left to dry for 24 hours. The plastic cone is open from both ends. The main purpose of the plastic cone is to give the MFC film its spherical shape, but also to prevent evaporated water vapor from escaping too quickly. This controlled evaporation prevents especially the film edges from shrinking too fast, thus reducing wrinkle formation into the film edges. A schematic view of the drying-setup is presented in Figure 2. The dried MFC film was then teared of from the PET substrate carefully. This fabrication method resulted homogeneous freestanding 28 cm diameter MFC films.

C. Fabrication of conducting patterns

Conducting patterns were fabricated on MFC film and PET reference film (as above) using screen printing technique from graphite ink (Loctite Edag PF 407C purchased from Afridana). Four different screens were used to obtain four different film thicknesses. Fabricated wet film thicknesses were 20, 40 80 and 120 µm. Two squares of size 2 cm x 2 cm were fabricated in the cases of all combinations of three different surfaces and four wet film thicknesses, resulting 24 patterns in total. Notice that in the case of MFC films, the patterns were printed on two different sides of the prepared films because the surface roughness was different on top side and bottom side due to the fabrication process. After screen printing the films were dried in convection over at 100 ºC for 1 hour.

D. Characterization of MFC films and conducting patterns

The MFC film and graphite electrode thicknesses were measured using digital micrometer screw (Insize 3101 Electronic Micrometer Screw). The film thicknesses where measured from three different positions from each film or pattern and from that data the average thickness and standard deviations were resolved.

A multimeter (Keithley 2002) and an in-house four-point probe were used in sheet resistance measurements. The four-probe technique applied here is described elsewhere in details [8]. Sheet resistance was measured from three different positions from each printed pattern. The four-point probe has four spring probes which are placed in line with equal spacing (s = 3 mm). Finally, the corrected sheet resistance is calculated from

$$R_S = G\frac{\pi}{\ln 2}\frac{V}{I}, \qquad (1)$$

where I is the applied current between the two outermost probes, V is the measured voltage between the two innermost probes and G is an additional geometric correction factor, which is determined by sample dimensions and the probe spacing [9]. The geometric factor for used square shaped (2 cm x 2 cm) patterns was $G = 0.86$.

Stylus profilometer (Bruker Dektak XT stylus profilometer) was used to characterize the surface topography of the prepared bare MFC films to obtain a

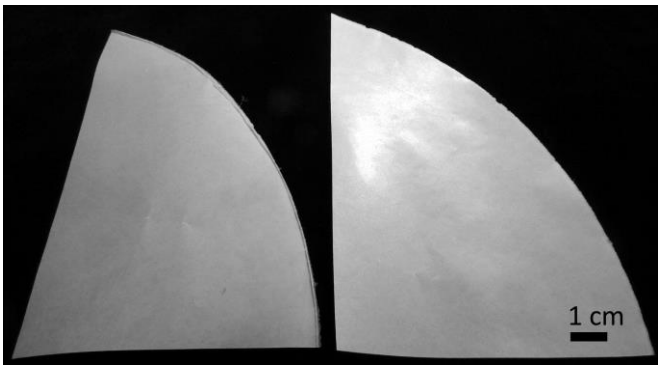

Figure 3*: Microscope images of top (left) and bottom (right) side surfaces of MFC film. These pieces were cut out from fabricated 28 cm diameter freestanding MFC film.*

surface roughness. Optical microscope (Zeiss Axio Imager A1) was used for optical characterization of MFC films.

III. Results and Discussion

A. Properties of MFC films

It can be observed clearly by naked eye, as well as from the different light reflection in the photograph shown in Figure 3, that MFC film roughness was very different on top side of the film in comparison to bottom side. This is resulting from the fabrication process where bottom side was in contact with flat PET film causing the relatively smooth surface on that side. On the other hand, the top side was in contact with air and due to high viscosity of MFC gel the surface did not settle smooth as in the case of water.

The profilometer topography curve for MFC top side surface is shown in the Figure 4. The profilometer analysis of MFC bottom side failed due to the non-successful attachment of MFC film using vacuum suction, which is most likely related to high roughness of the top side. Properties of PET and MFC films are shown in Table I.

TABLE I. The summary of MFC and PET film properties.

Thickness of MFC film (µm)	78.6 ± 0.6
Apparent density of MFC film (m^2/kg)	12.7
Roughness of MFC film (top side) (µm)	17.7
Thickness of PET film (µm)	125*
Density of PET (m^2/kg)	5.7*
Roughness of PET film (Ra) (nm)	30-40**

*Values obtained from Melinex ST506 Data Sheet.
**Values from reference [10].

Optical microscope images of MFC films are shown in Figure 5. The microfibers in the size scale of 20 µm are well visible on the bottom side surface (Figure 5a), whereas in the top side only some parts of the fibers are visible (Figure 5b). We interpret this so that on the bottom side the fibers have aligned into the to same horizontal plane along the PET substrate, whereas in the top size the fibers are more

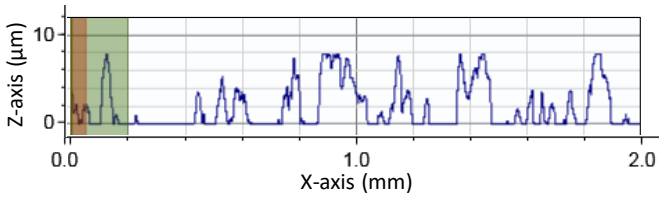

Figure 4*: Profilometer topography of top (rough side) surface of the MFC film.*

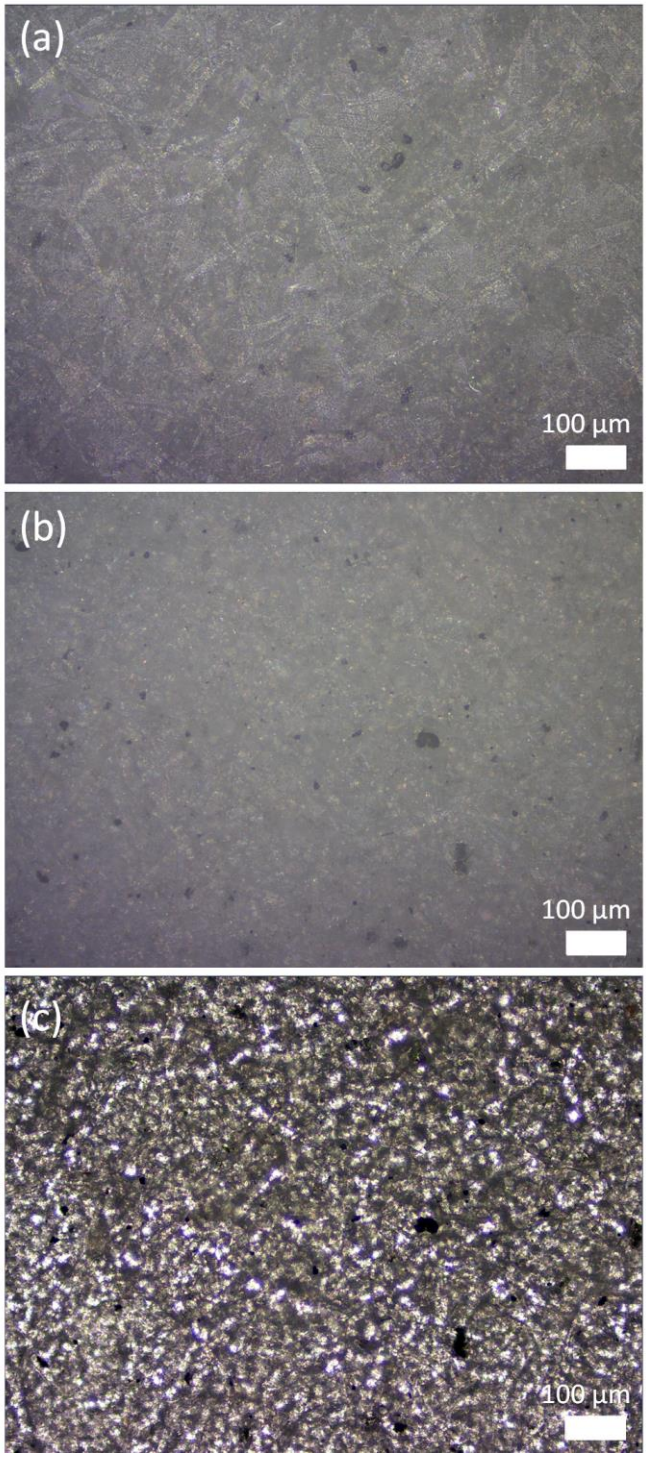

Figure 5: *Optical microscope images of MFC film from (a) bottom side (flat), (b) top side, and (c) in transillumination mode .*

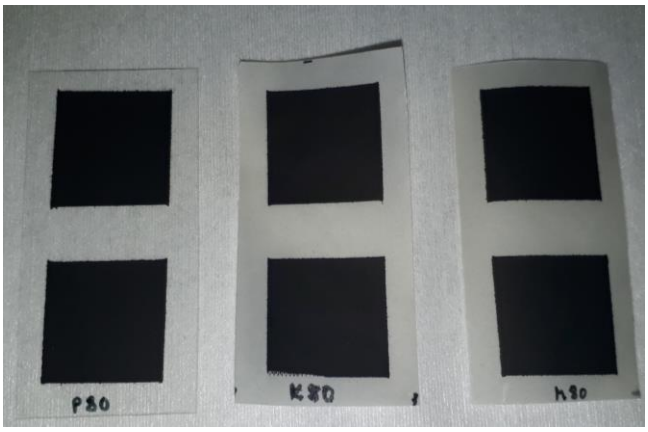

Figure 6: *Photographs of fabricated conducting graphite pattern on MFC and PET films.*

randomly oriented and thus only some part of them are visible in a certain focal plane.

B. Properties of conducting pattern on MFC film.

As an example, the set of graphite patterns obtained with 80 µm wet thickness of graphite ink using three different substrates are shown in Figure 6. In can be noticed that patterns are relatively homogeneous and pattern edges are quite smooth. There is some substrate curvature observe in the cases of MFC substrate, but the curvature was already present in the Figure 3 in the case of as-prepared MFC films.

The optical images of graphite patterns on MFC substrate are shown in the Figure 7. The graphite surfaces looks very flat without any indication of underlying fiber substrate. This indicated that the screen printing smoothens down the fiber structure roughness along with the ink deposition.

Results of the thickness and electrical conductivity measurements performed for graphite patterns are summarized in Table II. First of all, it can be noticed from thickness measurements that printed graphite film appear thinnest rough side of MFC film, and thickest on PET. This

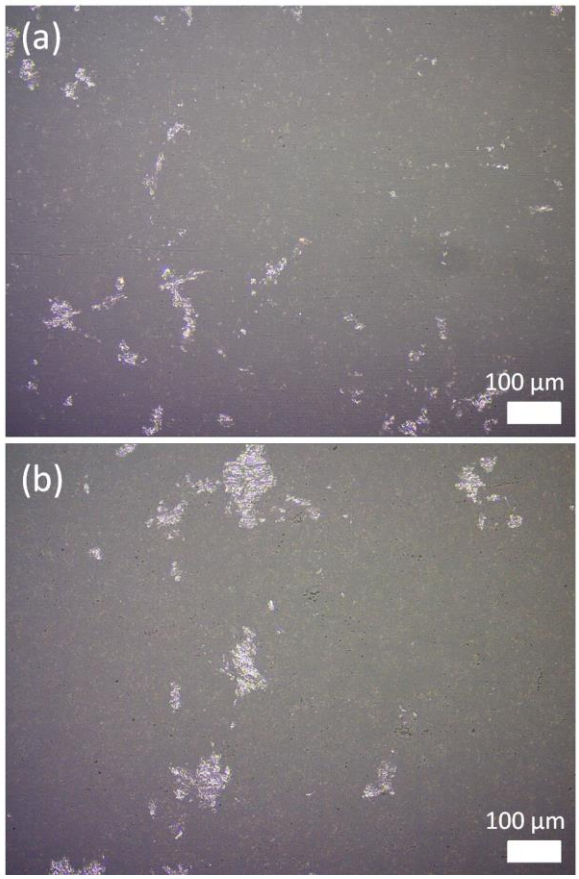

Figure 7*. Optical microscope images of dry graphite patterns on MFC substrate in the cases of (a) 40 and (b) 120 µm wet ink layer thicknesses.*

suggests that some material from the ink has absorbed into the MFC film, which is more porous than PET film. Also, as expected that larger wet thickness results into a thicker film. As can be seen from the Figure 8, the dry graphite layer thickness is almost linearly proportional to the wet graphite ink layer thickness, except in the case of the thinnest film.

As expected, the measured sheet resistances are lowest for the thickest films. Importantly, the sheet resistances in

TABLE II. THE SUMMARY OF GRAPHITE PATTERN PROPERTIES ON MFC AND PET FILMS.

Wet film thickness (µm)	**20**	**40**	**80**	**120**
Dry film thickness on MCF (top side) (µm)	4.5 ± 1.9	5.0 ± 2.4	13.6 ± 2.4	18.6 ± 1.7
Dry film thickness on MCF (bottom side) (µm)	8.9 ± 1.5	9.2 ± 1.3	17.1 ± 1.1	25.8 ± 2.2
Dry film thickness on PET (µm)	10.4 ± 1.1	14.6 ± 1.8	22.4 ± 0.9	32.2 ± 1.5
Sheet resistance on MFC (top side) (Ω/□)	55.2 ± 2.6	52.4 ± 5.0	18.4 ± 0.5	11.2 ± 0.9
Sheet resistance on MFC (bottom side) (Ω/□)	77.8 ± 1.7	50.8 ± 3.3	18.4 ± 1.1	13.0 ± 1.2
Sheet resistance on PET (Ω/□)	81.1 ± 1.8	56.2 ± 2.8	17.2 ± 0.4	11.2 ± 0.2
Conductivity on MFC (top side) (S/cm)	40.6 ± 1.9	38.2 ± 3.6	40.0 ± 1.0	48.2 ± 3.9
Conductivity on MFC (bottom side) (S/cm)	14.5 ± 0.3	21.4 ± 1.4	31.9 ± 1.8	29.7 ± 2.8
Conductivity of on PET (S/cm)	11.9 ± 0.3	12.2 ± 0.6	25.9 ± 0.6	27.8 ± 0.4

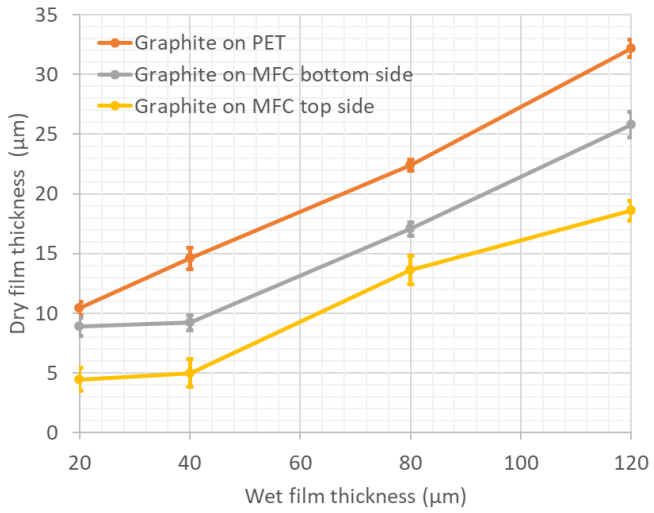

Figure 8*. Comparison of wet film thickness (with standard deviation bars) of graphite ink on with obtained final dry layer thickness in the cases of different substrates.*

the case of thickest film are the same in the case of PET and top side of MFC. In the case of thinnest film, top side of MFC gives clearly the lowest resistance.

The graphite film conductivities were calculated from the sheet resistance and thickness. Graphite pattern conductivities for different substrates and wet thicknesses are plotted in Figure 9. One can notice that top side MFC yields into the clearly highest conductivity values, whereas PET yields to lowest values. In the case of thinnest film, over two times higher conductivity. However, the high roughness of the top side of MFC film may cause some systematic error when using micrometer screw type layer thickness measurement, and thus the result can contain some uncertainty related to that.

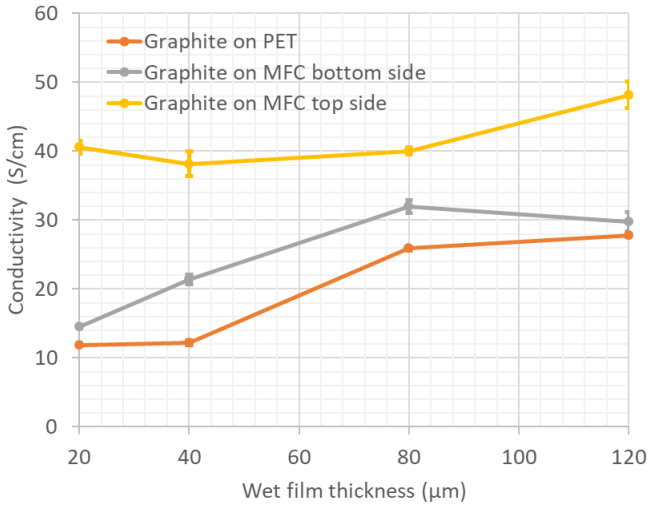

Figure 9*. Comparison of calculated conductivity (with standard deviation bars) of graphite film as a function of wet film thickness of graphite ink in the cases of different substrates.*

IV. Conclusion

In this paper, we have fabricated freestanding and robust films from microfibrillated cellulose and used those as substrates in screen printing process, where conducting patterns were fabricated from graphite ink. The electrical conductivity of printed patterns depended on the roughness of MFC film surface. We demonstrated here that nanocellulose or MFC are well suitable materials which could replace the oil based plastic substrates in the future and support the movement towards sustainable and green electronics.

References

[1] K. Torvinen, S. Lehtimäki, J. T. Keränen, J. Sievänen, J. Vartiainen, E. Hellén, D. Lupo, S. Tuukkanen, ”Pigment-Cellulose Nanofibril Composite and Its Application as A Separator-Substrate in Printed Supercapacitors”, *Electronic Materials Letters* 11(6) (2015) 1040-1047.

[2] J. Virtanen, J. Keskinen, A. Pammo, E. Sarlin, and S. Tuukkanen, ”Pyrolysed cellulose nanofibrils and dandelion pappus in supercapacitor application”, *Cellulose* 24(8) (2017), 3387.

[3] S. Rajala, T. Siponkoski, E. Sarlin, M. Mettänen, M. Vuoriluoto, A. Pammo, J. Juuti, O. J. Rojas, S. Franssila, and S. Tuukkanen, ”Cellulose nanofibril film as a piezoelectric sensor material,” *ACS Appl. Mater. Interfaces*, vol. 8(24), pp. 15607–15614, May 2016.

[4] R. Mangayil, S. Rajala, A. Pammo, E. Sarlin, J. Luo, V. Santala, M. Karp, and S. Tuukkanen, ”Engineering and Characterization of Bacterial Nanocellulose Films as Low Cost and Flexible Sensor Material”, *ACS Appl. Mater. Interfaces*, 9(22) (2017) 19048.

[5] A. Hänninen, E. Sarlin, I. Lyyra, T. Salpavaara, M. Kellomäki, S. Tuukkanen, ”Nanocellulose and chitosan based films as low cost, green piezoelectric materials”, *Carbohydrate Polymers* 202 (2018) 418.

[6] K. M. A. Uddin, V. Jokinen, F. Jahangiri, S. Franssila, O. J. Rojas, S. Tuukkanen, ”Disposable Microfluidic Sensor Based on Nanocellulose for Glucose Detection”, *Global Challenges*, 1800079, Nov. 2018.

[7] V. Kunnari, J. Pere, J. Hiltunen, K. Kemppainen, "Method of producing films from high consistency enzyme fibrillated nanocellulose", U.S. Patent Application No. 16/066,687, 2019.

[8] S. Tuukkanen, T. Julin, V. Rantanen, M. Zakrzewski, P. Moilanen, K. E. Lilja and S. Rajala, “Solution-processible electrode materials for a heat-sensitive piezoelectric thin-film sensor”, *Synthetic Met.*, vol. 162, pp. 1987-1995, 2012.

[9] H. Topsoe, “Geometric correction factors in four- point resistivity measurement”, *Bulletin no.* 472-13, 1968. Available online at: http://www.fourpointprobes.com/haldor.html (accessed 5 May 2014).

[10] K. A. Sierros. “Mechanical properties and characterisation of substrates for flexible displays”, Doctoral dissertation, University of Birmingham, 2006.